

Preparation and study of the physical properties of the ferrite compound $Al_{1-x}Zn_xFe_2O_4$ using sol gel method

Fares. A. Yasseen
 Department of Physics
 University of Kufa, *Najaf, Iraq*
Fares.alkufy@uokufa.edu.iq

Mohammed Abdul Ammer AL-Shareefi
 Department of Physics
 University of Babylon, *Babil, Iraq*

Abstract- In this research, we will prepare spinel ferrite (Zinc ferrite) by (Sol-Gel) a method, then we will depose it with Trivalent elements Aluminum, with a ratio of ($x = 0, 0.5, 0.7, 1.0$) to be with following formulas $Al_{1-x}Zn_xFe_2O_4$. After preparation of the samples we will study the structural properties of the compounds using X-ray diffraction (XRD), energy dispersive X-ray (EDX), and field emission scanning electron microscopy (FE-SEM), as well as using Fourier-transform infrared spectroscopy (F.T.I.R) to locate the atom in the crystal structure to find the type of ferrite. Then we will use Magnetic hysteresis will be measured using A vibrating-sample magnetometer (V.S.M.) to estimate the hysteresis loop of magnetism. XRD studies confirm that all the samples show a single-phase cubic spinel structure. The crystallite size of $Al_{1-x}Zn_xFe_2O_4$ calculated using the Debye-Scherrer formula was found in the range of (32-38). The value of the lattice parameter 'a' is found to decrease with increasing Al^{3+} content. EDX patterns confirm the compositional formation of the synthesized samples. FE-SEM micrographs show that all the samples have nano-crystalline behaviour and particles show spherical shape. The shapes show the magnetic behaviour of the prepared compound and other magnetic factors.

Keywords: Ferrites, Sol-Gel method, Nanoparticle, Crystal morphology, VSM.

I. INTRODUCTION

Ferrite is a chemical compound consisting of iron oxide (Fe_2O_3) or with one or several added metal elements. The chemical formula of ferrite is AFe_2O_4 , where A refers to any of the different metal cations [1].

Ferrite is considered not well conductive and is classified as ferromagnetic material. They are divided into two types (soft and hard) according to their resistance to being magnetic and compulsive force magnetism. Soft layers are characterized by low coercion, so it is easy to demagnetize.

Ferrite is used in the electronics industry to create inductors and transformers hearts and in various microwave components. While solid ferrite is characterized by extreme coercion and therefore difficult to demagnetize, it is used to make permanent magnets, for devices such as refrigerator magnets, speakers and electric motors [2].

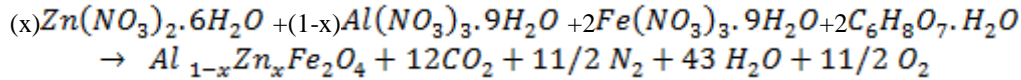
Spinel ferrite with the formula AB_2O_4 , where A and B represent different metal cations, usually containing Fe. Crystalline stenosis in the spinel layer usually consists of packing cubes (FCC). The structure of ferrite spinel is based on cations that occupy the price of tetrahedral and interfacial cations that occupy half of the octahedral openings divided into reverse spinel structure and natural spinel ferrite knew as "Zn Fe" contains the formula $ZnFe_2O_4$, with Fe^{3+} occupying octahedral sites and Zn^{2+} occupying positions Tetrahedral[3].

The aim of this research was to obtain Zinc ferrite nanopowder and adopted with aluminium by Sol-Gel method to study its physical properties.

II. EXPERIMENTAL

The reactive equation was calculated to calculate the molar weight masses of the reactants for the production of the ferrite compound $A_{1-x}Zn_xFe_2O_4$.

This process can be represented by the following equation:-

Table -1 shows the weights used for the preparation of the composite $Al_{1-x}Zn_xFe_2O_4$

No. of mole	$Fe(NO_3)_3 \cdot 9H_2O$	$C_6H_8O_7 \cdot H_2O$	$Zn(NO_3)_2 \cdot 6H_2O$	x	$Al(NO_3)_3 \cdot 9H_2O$	1-x	$2Fe(NO_3)_3 \cdot 9H_2O$	$2C_6H_8O_7 \cdot H_2O$
1	404.024	210.14	297.496	0	375.13	1	808.04	420.28
				0.5		0.5		
				0.7		0.3		
				1		0		

Preoperational hematite material's characterization

The Sol-Gel technique method was used here for preparation of hematite $Al_{1-x}Zn_xFe_2O_4$ with different values ($x = 0.0, 0.5, 0.7, 1$) with zinc ferrite nanoparticles to produce Nanocomposite.

Re weighed and placed in a thermal baker was added distilled water free of ions and the solution was placed on a Magnetic stirring At 50 ° C is added ammonia to the solution to change the solution PH and then the temperature is gradually increased until the solution becomes gel where it starts When the combustion is complete, its shape is loose, crisp and fluffy. The powder is then placed in a ceramic that bears the heat inside a carbolite oven and at a temperature of 600 degrees for 6 hours or so-called calcination and left to cool for 24 hours in the oven and then extracted and grinded again and returned to the oven and heat at a temperature of 1100 degrees for 6 hours or what is known as sintering and also left in the oven to cool for 24 hours and re-grinding process and grind it again to become homogeneous and we have to examine the XRD to make sure to get the spinel phase.

2-1 Characterization of samples

Powder X-Ray Diffraction (XRD) patterns have been recorded using an X'Pert PW 3040/60 spectrophotometer with Cu-K α radiation ($\lambda = 1.54\text{\AA}$). The morphology and elemental analysis were carried out using Field Emission – scanning electron microscopy (FE-SEM) TESCAN MIRA3 model with an EDX attachment. (TEM), operated at 120 Kv and equipped with a CCD camera was employed to record the micrographs of the synthesized samples. We used Infrared technology to determine the molecular structure of the prepared compounds and the ALPHA-BRUKER device. The magnetic properties were measured with a Vibrating Sample Magnetometer (Model 7400 VSM USA).

III. Results and discussion

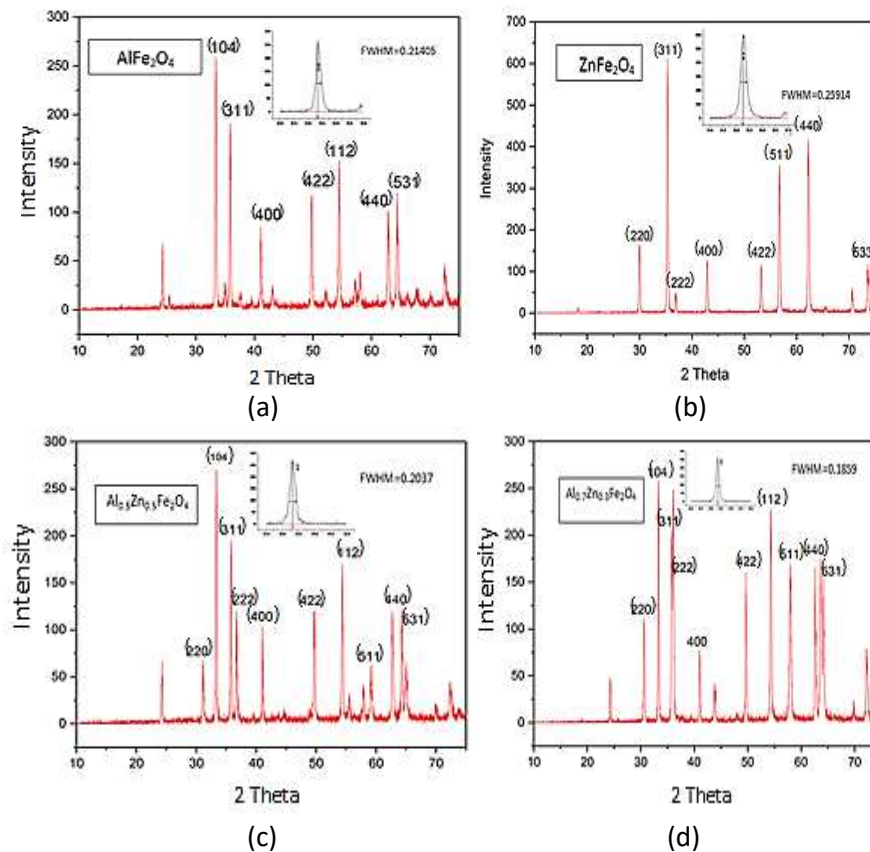
3.1 XRD studies

It was found that the pure composite $ZnFe_2O_4$ impregnated with aluminium in different proportions as polycrystalline in the preferred direction (311). The ferrite compound is smaller than $ZnFe_2O_4$ because the ionic diameter of aluminium is smaller than zinc, Any decrease in the interfacial distance of d_{hkl} surfaces as well as increased density of dislocations led to the shrinkage of the crystal and consequently the crystallization of its scale Table2.

Table -2 Grain size for the compound $Al_{1-x}Zn_xFe_2O_4$

compounds	(hkl)	Peak position (2 Theta)	FWHM	Crystallite size D (nm)	$\delta=1/D^2$	Dhkl (nm)	A(nm)
ZnFe ₂ O ₄	(311)	35.32995	0.2591	40.24412	0.000966113	0.2337419	0.077523438
AlFe ₂ O ₄	(104)	33.38976	0.2146	35.54632	0.000669425	0.2212821	0.09123696
Al _{0.5} Zn _{0.5} Fe ₂ O ₄	(104)	33.32085	0.2038	40.69688675	0.000603778	0.2208384	0.091054007
Al _{0.3} Zn _{0.7} Fe ₂ O ₄	(104)	33.34394	0.1859	44.60465727	0.00050262	0.2209870	0.091115314

The change of the direction of the crystal leads to a change in the crystal structure and therefore a change in the physical properties of the compound and this is reflected on other properties of the compound such as magnetism and electricity. From the distance between two atoms carrying opposite-magnetic azimuths and that the antimagnetic does not cause a radical change in the crystal structure but most often a reduction in the crystal symmetry as in the figure (1) [4].

Figure-1 X-Ray patterns of $Al_{1-x}Zn_xFe_2O_4$, a) AlFe₂O₄, b) ZnFe₂O₄, c) Al_{0.5}Zn_{0.5}Fe₂O₄, d) Al_{0.3}Zn_{0.7}Fe₂O₄

3.2 Field emission scanning electron microscope

The samples were examined using an FE-SEM device based on the ratio (X). When (X = 0.0) the ferrite compound takes the formula $Al_{1.0}Zn_{0.0}Fe_2O_4$ and when (X = 1) The compound takes the formula $Al_{0.0}Zn_{1.0}Fe_2O_4$, as in Figures (2a) and (2b), respectively, which shows the regular particle shape and gives a picture of the samples prepared at these proportions, where The crystal size of Aluminum frit is between (35.54-25-31)nm. As for the crystal size of zinc ferrite ranges between (40.24-25.54)nm, it is noted that the crystal size of zinc ferrite is larger than the Aluminum ferrite because the ionic radius of zinc is greater than the radius. Aluminum ion.[4]

The samples were examined according to the variable (X) ratio of the ferrite compound, where the decrease in the crystal size of the compound was observed $Al_{1-x}Zn_xFe_2O_4$. 2c, 2d) where the amount of increase in crystalline volume ranges from (40.24-29.19) nm The decrease in the crystalline size of the prepared particles is due to the aluminum ion that occupies the eight surface surfaces. The aluminum element at the eight-surface reticle sites leads to a decrease in the size of the nanoparticles, i.e., the particle rate increases as the zinc ion (Zn^{2+}) is replaced by the aluminum ion (Al^{3+}) in the crystalline lattice. Particle aggregation was observed for all prepared samples and their sizes were different, usually Nano scale. The results of the XRD assay match those obtained from FE-SEM.

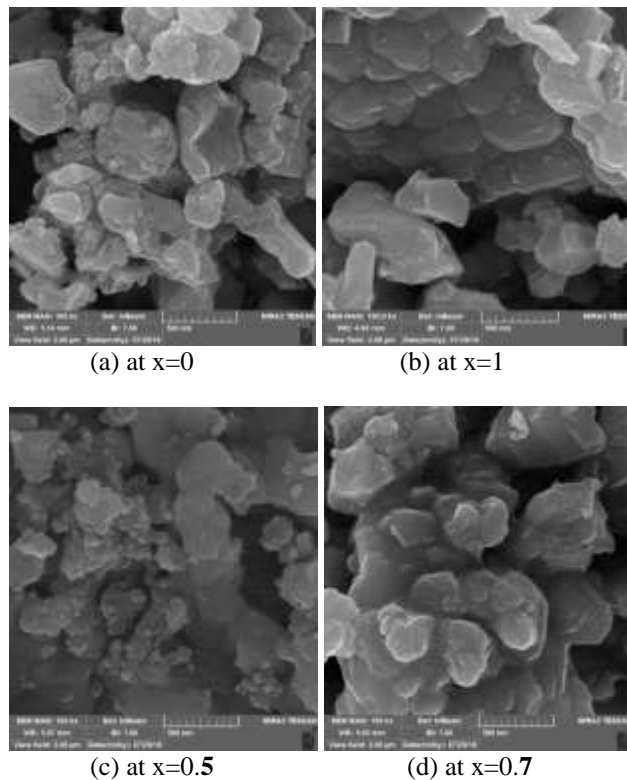


Figure-2 FESEM images of $Al_{1-x}Zn_xFe_2O_4$ with different ratios of Al a) $Al_{1.0}Zn_{0.0}Fe_2O_4$, b) $Al_{0.0}Zn_{1.0}Fe_2O_4$, c) $Al_{0.5}Zn_{0.5}Fe_2O_4$, d) $Al_{0.3}Zn_{0.7}Fe_2O_4$

3-3 Energy Dispersive X-Ray Spectroscopy (EDS)

This assay was used to determine the chemical elements of the ferrite compounds that were prepared.

This analysis showed the effect of (x) value of Al, Zn added to the ferrite compound $Al_{1-x}Zn_xFe_2O_4$ on the rest of its constituent elements, where between the EDS spectrum when (x) = 1 It contains only the following elements (iron, zinc and oxygen) as shown in Figure (3a), while Figure (3 b, c) shows the spectral analysis (EDS) for the percentages (X = 0.7,0.5,) shows the presence The following elements in the ferrite compound (aluminum, oxygen, zinc and iron), where we note the increase of aluminum by increasing ratio (x)

and decreasing zinc (high and low peaks) due to the substitution of aluminum as zinc components as there are no loss of the constituent elements of the Ferrite compound and for any prepared ratio. [5,6] Figure (3d), which represents the spectrum (EDS) of the ferrite compound prepared at $x = 0$ as it reveals the constituent elements of the compound including (iron, oxygen and aluminum) where no impurities were found and this indicates the purity of the samples and the success of the preparation method in our research. This is fully consistent with the results of XRD. [7].

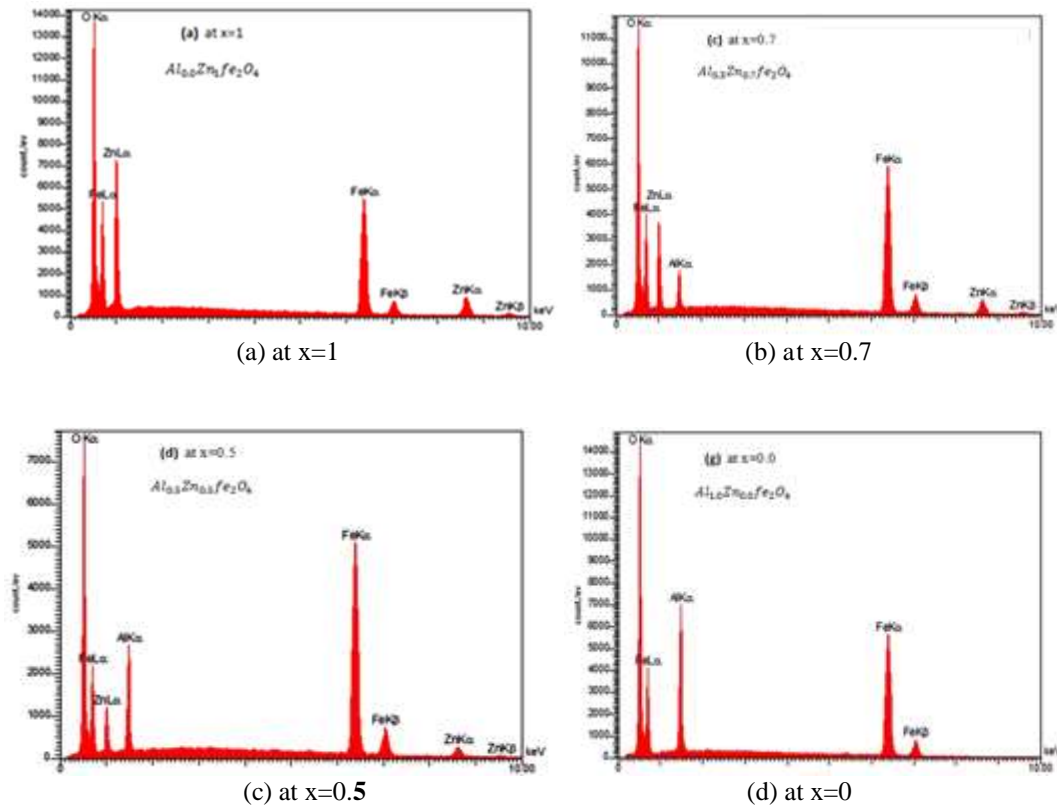


Figure-3 EDS for ferrite component $Al_{1-x}Zn_xFe_2O_4$ with different ratios of Al. a) $ZnFe_2O_4$, b) $Al_{0.3}Zn_{0.7}Fe_2O_4$, c) $Al_{0.5}Zn_{0.5}Fe_2O_4$, d) $AlFe_2O_4$

3-4 FTIR Analysis

FTIR technology has been used because it provides comprehensive information and rich experimental data to help the development and progress of the research. It is also an excellent tool for studying the distribution of cations in tetrahedral sites and octahedral sites in the Ferrite system and showing the characteristics and characterization of materials that are considered as human fingerprint.

The frequency range $(400-4000) \text{ cm}^{-1}$, which shows the infrared spectrum at room temperature, is shown in Figure 4, which shows the infrared spectrum of the $Al_{1-x}Zn_xFe_2O_4$ ferrite complex ($x = 0, 0.5, 0.7, 1$). Several bonds were observed through the FTIR spectrum between cm^{-1} (490-533) and the structural changes resulting from the metal ions that strongly influenced the reticle vibrations. These vibrations also depend on cations, oxygen ions and bonding strength.

The main vibrations also occur between the tetrahedral and octahedral sites resulting in red displacement at the peaks with the value (X) when they increase the aluminum ion due to the increase of this element's contribution to the electronic density of the oxygen-iron core. This increase led to a more red displacement of cadmium because it has the ability to The absorption of electron densities is equal or pushed evenly. Because the radius of aluminum is less than the radius of cadmium, the displacement for the aluminum ion is greater than the cadmium ion. This is evident from the results figure (4) [8].

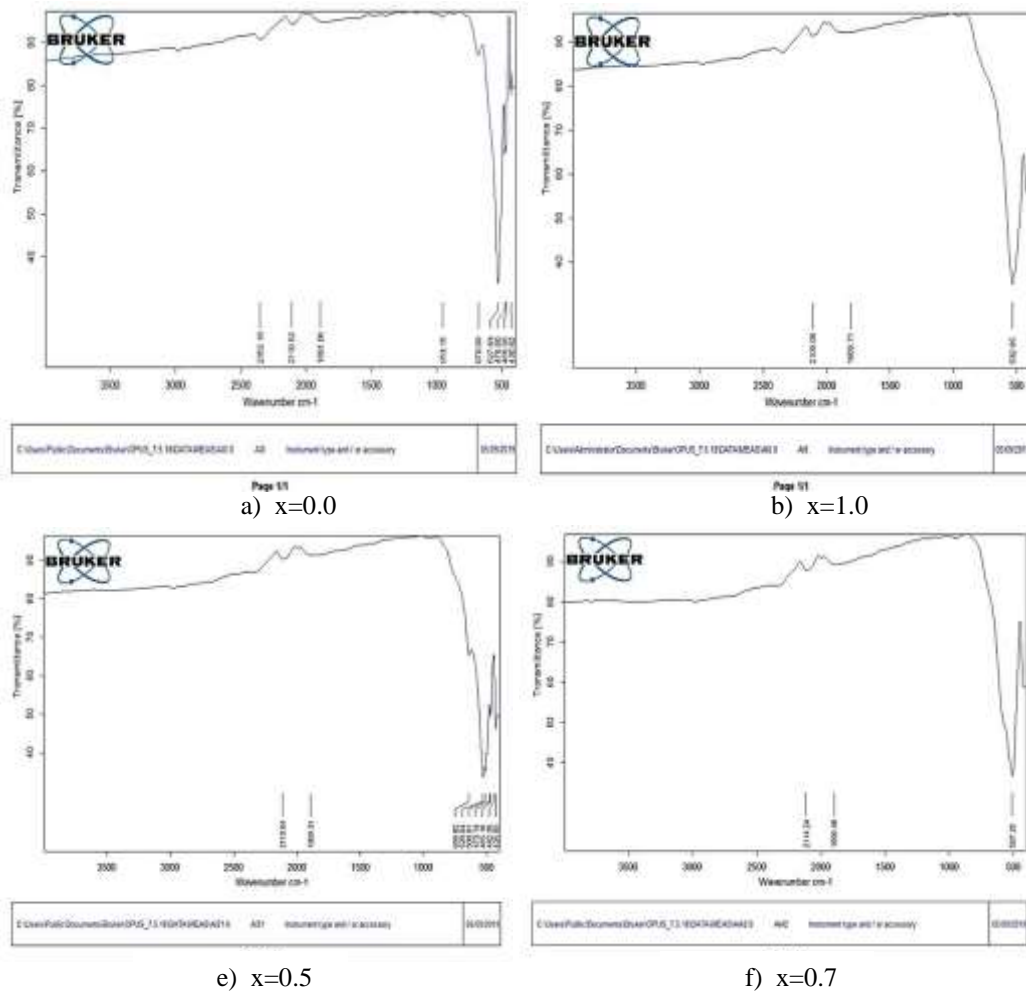


Figure-4 FTIR for ferrite component $Al_{1-x}Zn_xFe_2O_4$ with different ratios of Al. a) $AlFe_2O_4$, b) $ZnFe_2O_4$
 c) $Al_{0.5}Zn_{0.5}Fe_2O_4$, d) $Al_{0.3}Zn_{0.7}Fe_2O_4$

3-5 VSM test

Magnetic properties and magnetic field strength were studied using a device (Vibrating Sample Magnetometer) (VSM) at room temperature.

Figure 5 illustrates the hysterical loop of the $Al_{1-x}Zn_xFe_2O_4$ at ($x = 0, 0.5, 0.7, 1$) The figure shows the magnetic behavior of the prepared compound and magnetic factors such as M_s saturation magnetization, M_r residual magnetization and H_c .

The narrow curves indicate the properties of magnetism with spinel-free behavior, as the narrow hysterical ring indicates the loss of magnetism. Amount (x).[9,10,11].

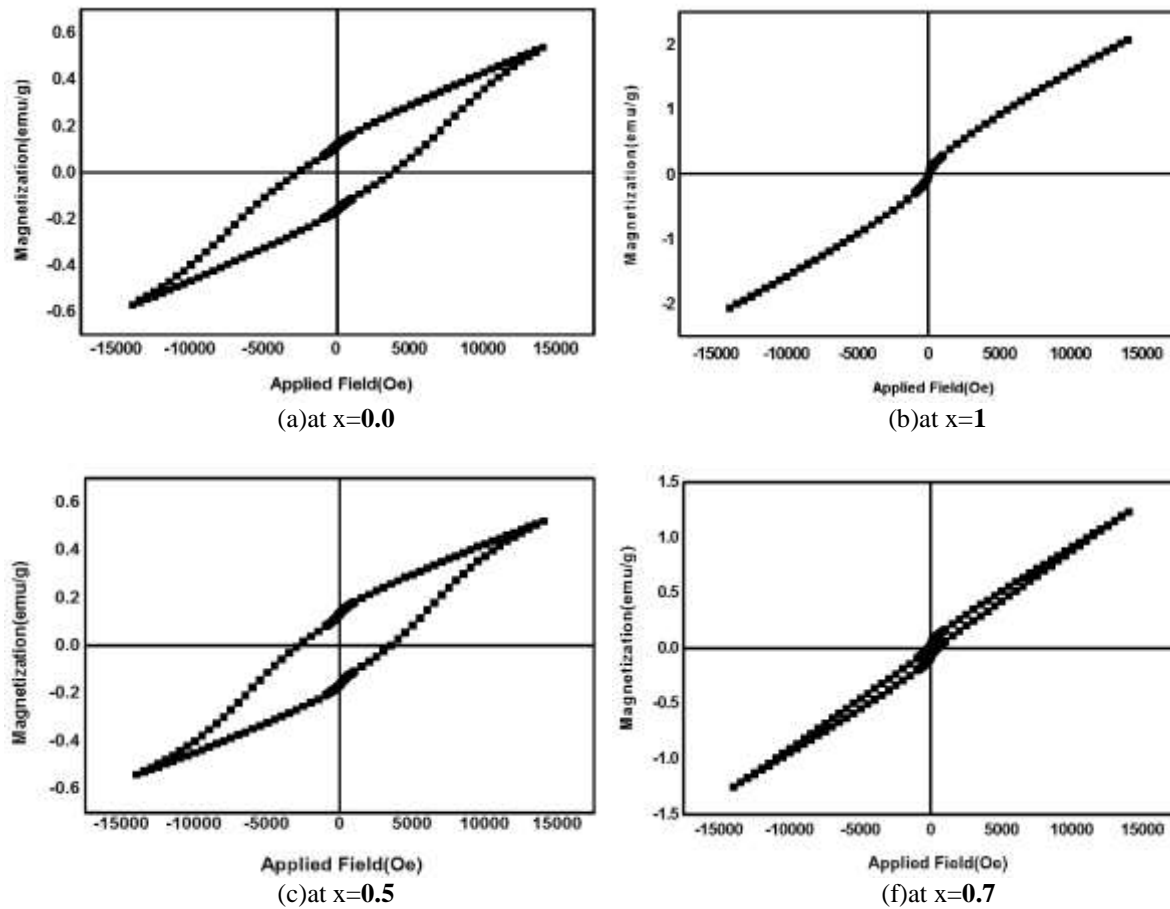


Figure-5 Magnetic hysteresis curves of $Al_{1-x}Zn_xFe_2O_4$ with different ratios of Al at sintering of 1100 °C for 6 hour. a) $AlFe_2O_4$, b) $Zn_{1.0}Fe_2O_4$, c) $Al_{0.5}Zn_{0.5}Fe_2O_4$, d) $Al_{0.3}Zn_{0.7}Fe_2O_4$

Table (3) shows the differences in all the saturation magnetic properties as well as differences in the other magnetic factors, as can be seen the decrease and increase in the saturation area of the ratio (X) as well as the difference with the residual magnetization for (X) and this is due to the size of the particles The shape and distribution of positive ions at tetrahedral sites and eight-surfaces sites and the cause of diminishing saturation magnetic is to rearrange the positions between the ions in addition to that the magnetic behavior of Al^{+3} ion less than Zn^{+2} ion and this is reflected in the force major increase when the proportion of Al^{+3} ion [10] As well as increasing the ratio (X) [11,9] This is indicated in the pure sample when $Al = 0.0$ and the increase in coercion may be due to the variation of the crustal magnetic and the exchange of properties due to the disruption of rotation on the surface of the molecules and the formation of the first non-magnetic phase [11].

Table-3 Magnetic saturation (Ms), remaining magnetism (Mr) and coercive force (Hc) as a function of cobalt ratio.

Sample	Component	Ms	Mr	Hc	Mr/Ms
X=1.0	$Al_{0.0}Zn_{1.0}Fe_2O_4$	2.072	0.01	10.052	0.004826255
X=0.7	$Al_{0.3}Zn_{0.7}Fe_2O_4$	1.235	0.053	365.823	0.04291498
X=0.5	$Al_{0.5}Zn_{0.5}Fe_2O_4$	0.867	0.074	1025.503	0.085351788
X=0.0	$Al_{1.0}Zn_{0.0}Fe_2O_4$	0.538	0.121	3702.985	0.224907063

IV . Conclusion

We have successfully synthesized $Al_{1-x}Zn_xFe_2O_4$ ($x=0.0, 0.5, 0.7, 1$) ferrite nanoparticles using Sol-Gel methods. XRD results indicate that all samples have a single-phase cubic spinel structure. Lattice parameters and crystallite size have been found to decrease with Al doping. FE-SEM micrographs show that all particles have spherical shape nano-crystalline behaviour. The infrared spectrum showed the presence of elements prepared through the vibration spectrum, which between several bonds of metal ions formed in the region is dependent on oxygen ion and bonding strength. The magnetic study infers that saturation magnetization, remnant magnetization and coercive field decreases with an increase in Al doping, which may be due to the dilution of the sub-lattice by nonmagnetic ions doping.

REFERENCES

- [1] C.B.Carter, and M. G. Norton, "Ceramic Materials Science and Engineering", 2nd ed. , Springer, 2013.
- [2] A.Okamoto , " The Invention of Ferrites and their Contribution to the Miniaturization of Radios ", IEEE, 2009.
- [3] P.W.Atkins, T.L.Overton, J.P.Rourke, M.T. Weller and F.A. Armstrong, " Inorganic Chemistry " , New York: W.H. Freeman, 2010.
- [4] M. Nasreddine, " X-ray and some applications " , Arab Atomic Energy Authority, Tunisia 2008.
- [5] A. S. Shaikat; et al" Effects of a Novel Poly (AA-co-AAm)/AlZnFe₂O₄/potassium Humate Superabsorbent Hydrogel Nanocomposite on Water Retention of Sandy Loam Soil and Wheat Seedling Growth", *Molecules* 2012, 17, 12587-12602; doi:10.3390/molecules171112587
- [6] K. Vijaya Kumar I et al , " " ,Effect of Aluminium Doping on Structural and Magnetic Properties of Ni-Zn Ferrite Nanoparticles, *World Journal of Nano Science and Engineering*, 2015, 5, 68-77
- [7] Samad Zare et al, Synthesis, "Structural and Magnetic behavior studies of Zn-Al substituted cobalt ferrite nanoparticles", *Journal of Molecular Structure* (2015), doi: <http://dx.doi.org/10.1016/j.molstruc.2015.02.006>
- [8] Sonal Singhal, et al, "Effect of Zn Substitution on the Magnetic Properties of Cobalt Ferrite Nano Particles Prepared Via Sol-Gel Route", *Journal of Electromagnetic Analysis and Applications* · January 2010 DOI: 10.4236/jemaa.2010.26049
- [9] N.M. Deraz, M.M. Hessien, "Structural and magnetic properties of pure and doped nanocrystalline cadmium ferrite", *Journal of Alloys and Compounds* 475 832–839. 2009.